

Surface Morphology Control of Polymer Films by Electron Irradiation and Its Application to Superhydrophobic Surfaces

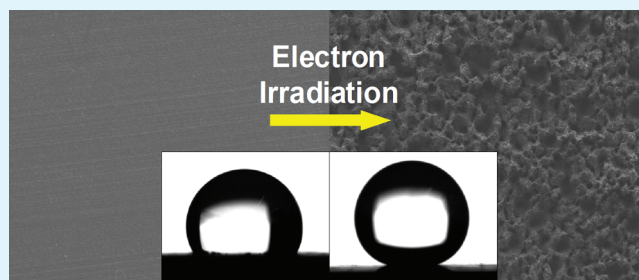
Eun Je Lee,[†] Chan-Hee Jung,[†] In-Tae Hwang,[†] Jae-Hak Choi,^{*,†} Sung Oh Cho,^{*,†} and Young-Chang Nho[†]

[†]Radiation Research Division for Industry and Environment, Advanced Radiation Technology Institute, Korea Atomic Energy Research Institute, Jeongeup-si, Jeollabuk-do 580-185, Republic of Korea

^{*}Department of Nuclear and Quantum Engineering, Korea Advanced Institute of Science and Technology, Daejeon 305-701, Republic of Korea

 Supporting Information

ABSTRACT: A simple and controllable one-step method to fabricate superhydrophobic surfaces on poly(tetrafluoroethylene) (PTFE) films is developed on the base of electron irradiation. When the thickness of PTFE films is higher than the penetration depth of electron beams, electrical charging occurs at the surface of the films because of the imbalance between the accumulation of incident electrons and the emission of secondary electrons. Local inhomogeneity of charge distribution due to this electrical charging results in the nonuniform decomposition of PTFE molecular bonds. As electron fluence increases, surface morphology and surface roughness of the films are dramatically changed. An extremely rough surface with micrometer-sized pores is produced on the surface of PTFE films by electron irradiation at a fluence higher than $2.5 \times 10^{17} \text{ cm}^{-2}$. Because of high surface roughness, the irradiated PTFE films exhibit superhydrophobic property with a water contact angle (CA) greater than 150° at fluences ranging from 4×10^{17} to $1 \times 10^{18} \text{ cm}^{-2}$. The surface morphology and corresponding water CA can be controlled by simply changing the electron fluence. This electron irradiation method can be applicable to the fabrication of superhydrophobic surfaces using other low-surface-energy materials including various fluoropolymers.



KEYWORDS: electron irradiation, PTFE, superhydrophobic, charging effect, porous structure, contact angle

INTRODUCTION

The wetting property is one of the most important properties of a material surface. The wetting property of a material surface is determined by two factors, the surface roughness and surface energy of the material;¹ thus, the wetting property of a surface can be tuned by controlling the surface roughness and surface energy. Recently, the fabrication of superhydrophobic surfaces, which result from the combination effect of high surface roughness and low surface energy, has attracted a great deal of attention because superhydrophobic surfaces have unique properties including self-cleaning, antiadhesion, and antioxidation.^{2–4}

As a precursor material for the fabrication of superhydrophobic surfaces, poly(tetrafluoroethylene) (PTFE) has been used because of its intrinsic low surface energy and excellent properties such as chemical resistance, high temperature stability, electrical insulation, and a low coefficient of friction.^{5,6} Various fabrication methods using PTFE have been developed, including a template method,⁷ extension,⁸ physical vapor deposition,^{9–11} electrospraying,^{12,13} and irradiation methods.^{14–17} Among these methods, irradiation methods have the advantages of a one-step process and easy large-area production for real applications. Although irradiation methods including ion implantation,^{14,15} O₂ RF plasma treatment,¹⁶ and synchrotron radiation¹⁷ have been developed, they have some disadvantages. Because the

penetration depth of ion beam and plasma irradiation is at most a few μm , only the near surface region of a material is transformed using these methods, and thus, it is difficult to modify the entire target materials. In addition, the synchrotron radiation exhibits an intrinsic broad energy spectrum, which might result in non-uniform modification. However, an electron beam has uniform beam energy and, moreover, the penetration depth of an electron beam is at least several tens of times longer than that of an ion beam or plasma at the same energy level. Furthermore, the electron irradiation technique is known to be a simple process for the fabrication of rough surface structures, which are essential for the superhydrophobicity.^{18,19}

Here, we present a facile and straightforward route to control the morphology of PTFE films and to fabricate superhydrophobic surfaces by using electron irradiation. The irradiated PTFE films were characterized using field emission scanning electron microscopy, X-ray photoelectron spectroscopy, and contact angle measurement. The irradiated PTFE films exhibited a rough surface structure with micrometer-sized pores and a superhydrophobic property at an adjusted electron fluence.

Received: April 14, 2011

Accepted: July 21, 2011

Published: July 21, 2011

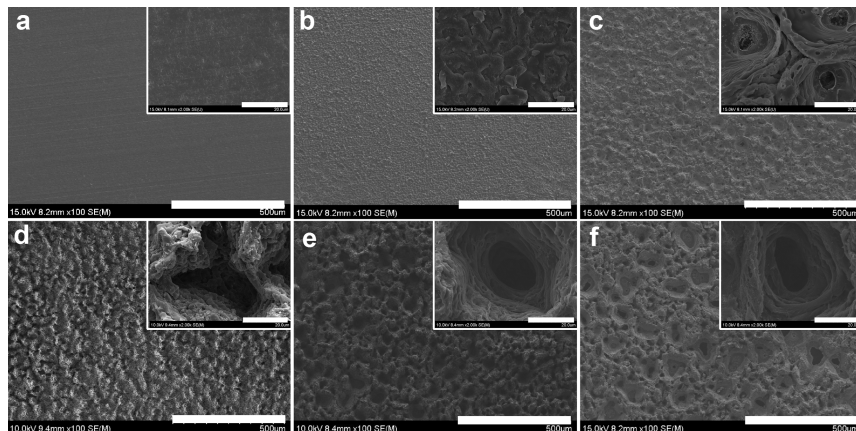


Figure 1. FESEM images of the (a) pristine and electron-irradiated PTFE films at electron fluences of (b) 5×10^{16} , (c) 2.5×10^{17} , (d) 4×10^{17} , (e) 6×10^{17} , and (f) $1 \times 10^{18} \text{ cm}^{-2}$, respectively (scale bars, 500 μm). The insets show the corresponding magnified FESEM images (scale bars, 20 μm).

■ EXPERIMENTAL SECTION

PTFE films (Universal Co., Ltd., Japan) with thicknesses of 50 and 100 μm were used as precursor materials. The PTFE films were fixed on Si wafer substrates (2 cm \times 2 cm) using conductive carbon tape. The PTFE films were irradiated with an electron beam generated from a thermionic electron gun.²⁰ The electron irradiation process was carried out at room temperature in a vacuum chamber under a pressure of less than 2×10^{-5} Torr. The energies of the electron beams irradiating the films were 30 and 50 keV, and the current density of the beams was about 8 $\mu\text{A}/\text{cm}^2$. The total electron fluence of the electron beams irradiating the samples was varied from 5×10^{16} to $2 \times 10^{18} \text{ cm}^{-2}$ by changing the irradiation time. During the irradiation, the sample substrate was water-cooled to reduce the heat produced by the electron irradiation. Charging and breakdown phenomena during the irradiation process were recorded using a CCD camera.

The morphologies of the pristine and electron-irradiated PTFE films were characterized using a field-emission scanning electron microscope (FESEM, Hitachi S-4800) and a 3D optical surface profiler (Nano System Co. Ltd., NV-2000). The chemical compositions of the pristine and electron-irradiated PTFE films were investigated by X-ray photoelectron spectroscopy (XPS) using a Mg and Al K α X-ray source in a SIGMA PROBE (Thermo VG) spectrometer. The XPS spectra were curve-fitted with a mixed Gaussian–Lorentzian shape using the analysis software of XPSPEAK.²¹ Shirley function was used to remove the background prior to curve fitting. All the XPS spectra were charge-compensated to C 1s at 285.0 eV.^{22,23} The wetting property of the film was analyzed based on the water contact angle (CA) measured using a CA measurement system (SEO Co., Ltd., Phoenix 300 Plus). The volume of a water drop used for the CA measurement was 4 μL . Sliding angle (SA) measurement was performed by using an apparatus made by ourselves.

■ RESULTS AND DISCUSSION

The color of pristine PTFE film (thickness: 100 μm) was translucent white but turned into brown after electron irradiation. Figure 1 displays the morphological change of the PTFE films induced by the electron irradiation at an electron fluence up to $1 \times 10^{18} \text{ cm}^{-2}$. The surface of the pristine PTFE film exhibited relatively negligible surface roughness (Figure 1a). After electron irradiation at an electron fluence of $5 \times 10^{16} \text{ cm}^{-2}$, the surface of the PTFE film became bumpy, as shown in Figure 1b, and thus, surface roughness slightly increased compared with that of the pristine film. At an electron fluence of $2.5 \times 10^{17} \text{ cm}^{-2}$, the

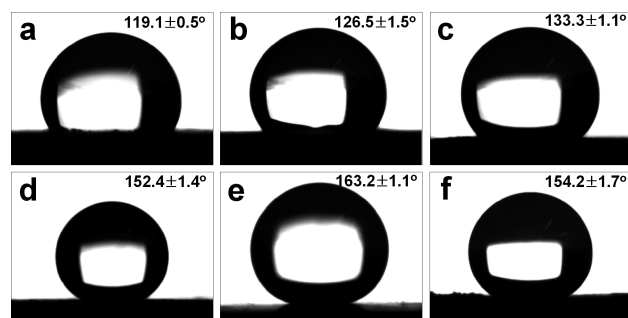


Figure 2. Water contact angles measured before and after electron irradiation at different electron fluences: (a) 0; (b) 5×10^{16} ; (c) 2.5×10^{17} ; (d) 4×10^{17} ; (e) 6×10^{17} ; (f) $1 \times 10^{18} \text{ cm}^{-2}$.

surface structure of the film was changed as shown in Figure 1c. Interestingly, many micrometer-sized pores with a diameter of about 8 μm were produced. In addition, the surrounding area of the micrometer-sized pores became crumpled. When the electron fluence was further increased to 4×10^{17} and $6 \times 10^{17} \text{ cm}^{-2}$, the size and depth of the pores were increased to more than 20 μm and the number of pores was also gradually increased (Figure 1d,e). After electron irradiation at a further increased electron fluence of $1 \times 10^{18} \text{ cm}^{-2}$, larger pores were produced as a result of the collapse and mergence of some pores as shown in Figure 1f. Electron irradiation at an electron fluence of more than $1 \times 10^{18} \text{ cm}^{-2}$ did not further change the surface morphology. Though the electron fluence increased to $2 \times 10^{18} \text{ cm}^{-2}$, the morphology was almost the same as a surface irradiated at an electron fluence of $1 \times 10^{18} \text{ cm}^{-2}$ (see Figure S1 in the Supporting Information). This result indicates that the morphologies of the PTFE surfaces could be changed by adjusting the electron fluence within a certain range.

In addition to the FESEM analysis, we investigated the surface morphology using a 3D optical surface profiler, which can provide a 3D morphology with a much large area in comparison to an atomic force microscope. The surface profiles of the pristine and electron-irradiated PTFE films are shown in Figure S2 (see the Supporting Information). The average depth of the pores is about 65 and 75 μm at electron fluences of 4×10^{17} and $6 \times 10^{17} \text{ cm}^{-2}$, respectively. The pristine PTFE film exhibited a root-mean-square (rms) roughness of $259.93 \pm 12.11 \text{ nm}$. As the

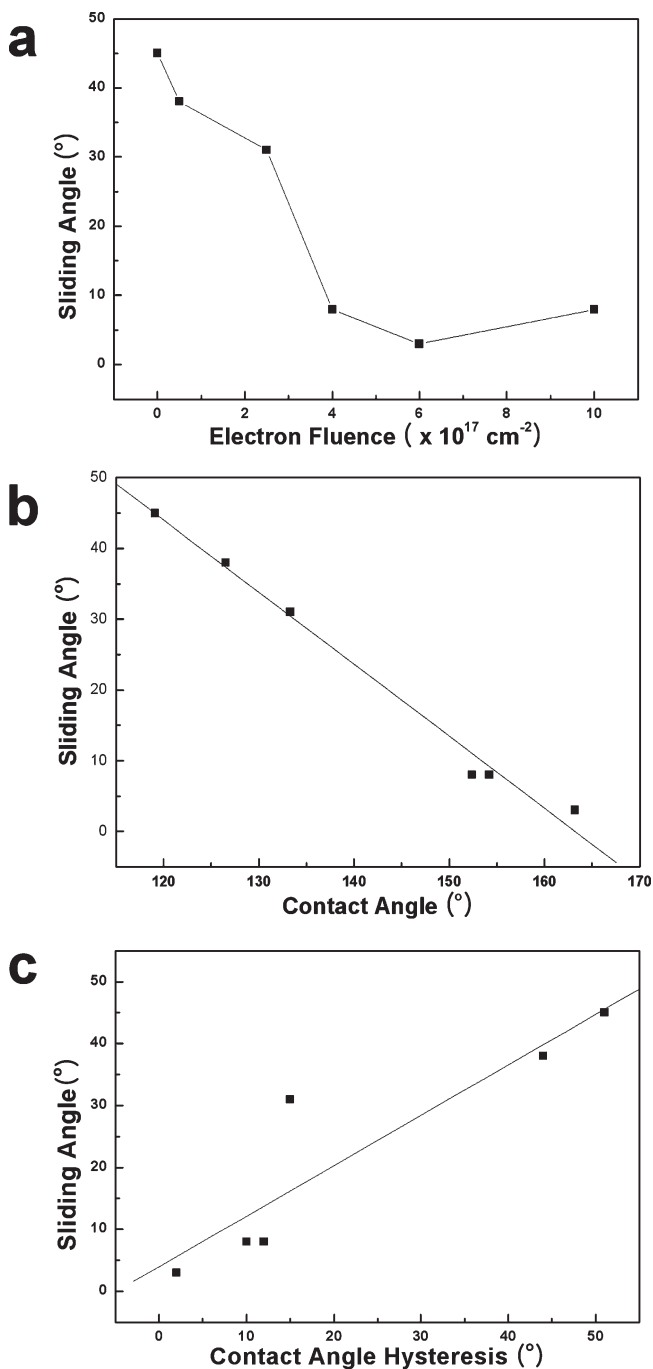


Figure 3. Sliding angles as a function of (a) the electron fluence, (b) dependence of the sliding angle on the contact angle, and (c) contact angle hysteresis.

electron fluence increased, the rms roughness of the irradiated films was gradually increased to $30.09 \pm 0.94 \mu\text{m}$.

The formation mechanism of such a structure could be explained in terms of the inhomogeneous decomposition of the PTFE film caused by the charging effect. Electrical charging and breakdown phenomena were observed when the irradiated PTFE film was monitored using a CCD camera. Many points on the PTFE film were brighter than other parts of the film and continuously flashed (see movie file in the Supporting Information). Because PTFE is an electrically insulating polymer

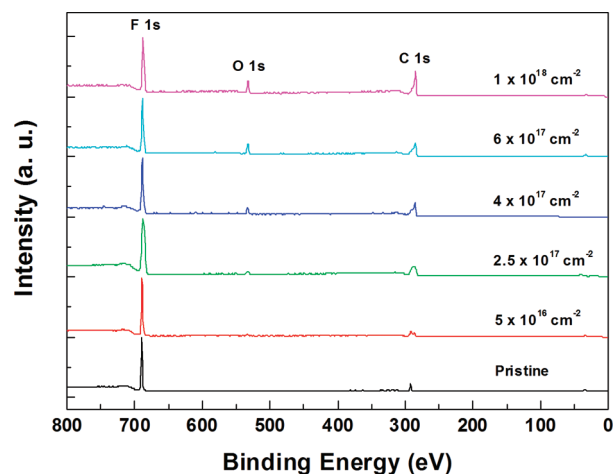


Figure 4. XPS survey spectra of the (a) pristine and electron-irradiated PTFE films at electron fluences of (b) 5×10^{16} , (c) 2.5×10^{17} , (d) 4×10^{17} , (e) 6×10^{17} , and (f) $1 \times 10^{18} \text{ cm}^{-2}$.

and the penetration depth of a 30-keV electron beam into PTFE is about $10 \mu\text{m}$ (see Figure S3 in the Supporting Information), PTFE films thicker than $10 \mu\text{m}$ tend to be charged if electron-irradiated. When the PTFE film is irradiated with an electron beam under the above conditions, incident electrons are mainly trapped in the film or backscattered, and secondary electrons are emitted from atoms comprising the PTFE. In the case of 30-keV electron irradiation of PTFE, the backscattered and secondary electron yields are 0.077 and 0.105, respectively.²⁴ Because the sum of the backscattered and secondary electron yields is less than unity, the PTFE films became increasingly negatively charged as the electron irradiation proceeds, and thus, the surface potential increases gradually. If the surface potential reaches the discharge inception value, breakdowns occur at weak points in the PTFE film.²⁴ For a comparison, an experiment for reducing the charging effect was carried out using a different sample under different irradiation conditions. When the film thickness was reduced from 100 to $50 \mu\text{m}$ and the electron beam energy was increased from 30 to 50 keV, which led to a corresponding penetration depth of electrons into PTFE of about 2.5 times longer than that of 30-keV electrons (see Figure S3 in the Supporting Information), the charging intensity was dramatically reduced and was rarely observed under these conditions. Although the electron fluence reached to $6 \times 10^{17} \text{ cm}^{-2}$, the irradiated surface became only slightly roughened and micrometer-sized pores were rarely found compared with the morphology shown in Figure 1e (see Figure S4 in the Supporting Information).

On the basis of the above experiments, we can conclude that the electrical charging is a key parameter to induce a morphological change. Due to the charging effect, the local inhomogeneity of charge distribution is induced: some local regions of the PTFE film becomes negatively charged so that other regions of the PTFE film become relatively positive. In such circumstances, the relatively positive part attracts more electrons of the beam because electrons are negatively charged particles. As a result, the decomposition induced by the electron irradiation becomes inhomogeneous over the film and relatively positive regions of the PTFE undergo more intensive decomposition, which finally induces the formation of micrometer-sized pores.

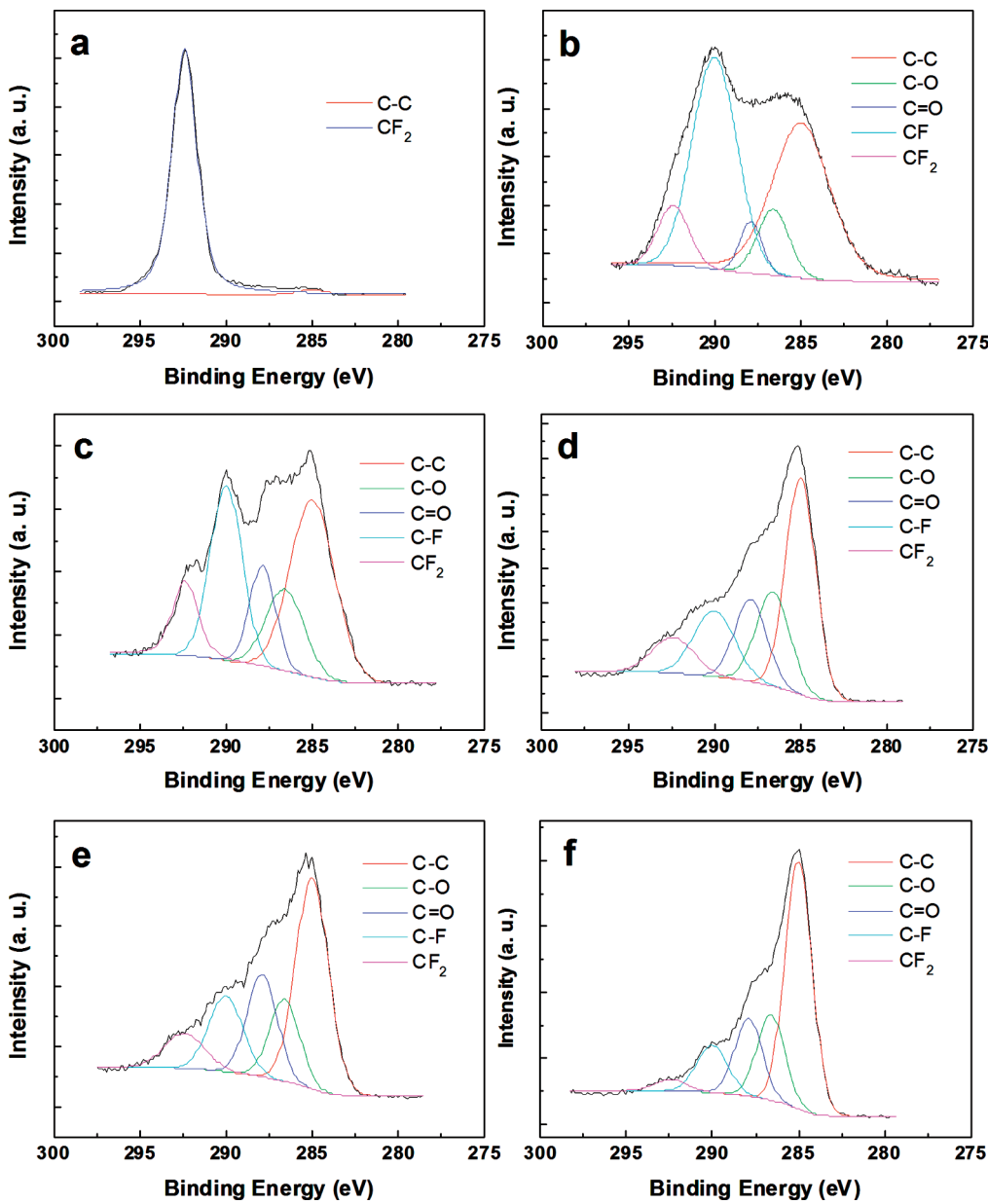


Figure 5. XPS C 1s peaks of the (a) pristine and electron-irradiated PTFE films at electron fluences of (b) 5×10^{16} , (c) 2.5×10^{17} , (d) 4×10^{17} , (e) 6×10^{17} , and (f) $1 \times 10^{18} \text{ cm}^{-2}$.

The wetting property of the pristine and electron-irradiated PTFE films was evaluated by measuring their water contact angles (CAs) (Figure 2). The pristine PTFE film showed a CA of $119.1 \pm 0.5^\circ$, indicating that the surface was hydrophobic. As the electron fluence increased, the CA of the irradiated surface gradually increased. The surface began to show a superhydrophobic property with a CA of $152.4 \pm 1.4^\circ$ at an electron fluence of $4 \times 10^{17} \text{ cm}^{-2}$, and the surface exhibited a maximum CA of $163.2 \pm 1.1^\circ$ when the electron fluence was $6 \times 10^{17} \text{ cm}^{-2}$. However, electron irradiation at an electron fluence of more than $6 \times 10^{17} \text{ cm}^{-2}$ resulted in a decrease in CA. For example, the CA decreased from $163.2 \pm 1.1^\circ$ to $154.2 \pm 1.7^\circ$ when the electron fluence increased from 6×10^{17} to $1 \times 10^{18} \text{ cm}^{-2}$.

Furthermore, the sliding angles (SAs) and CA hysteresis, which is the difference between advancing and receding angles, of the films were measured. When the electron fluence was less

than $2.5 \times 10^{17} \text{ cm}^{-2}$, water droplets were pinned to the surfaces of the pristine and electron-irradiated PTFE films, and thus, they were not easily detached. On the contrary, the electron-irradiated films at a fluence higher than $4 \times 10^{17} \text{ cm}^{-2}$ showed the SAs of less than 10° . The film irradiated at an electron fluence of $6 \times 10^{17} \text{ cm}^{-2}$ exhibited the lowest SA of about 3° (Figure 3a). The SA linearly decreased as the CA increased as shown in Figure 3b. When the hydrophobic surface of the film was converted to a superhydrophobic one by increasing the electron fluence, both the CA and SA were remarkably changed. A remarkable decrease of the SA and increase of the CA might be accompanied by the transition between the Wenzel state and the Cassie state,²⁵ which are explained in detail below. The relationship between the SA and CA hysteresis is exhibited in Figure 3c, and a linear relation similar to the Yoshida et al.'s report was shown.²⁶ When the CA hysteresis increased, the SA also increased. Thus, we can

conclude that CA hysteresis, SA, and CA are closely related, although the former two properties describe dynamic wetting, while the latter property describes static wetting.

To explain the behavior of CA change, the chemical composition change was investigated using X-ray photoelectron spectroscopy (XPS) because the wetting property is determined not only by the morphology but also by the surface chemistry. In the XPS survey spectra, the pristine PTFE film showed only carbon (C) and fluorine (F) peaks. However, an oxygen (O) peak appeared after the electron irradiation and the content of the O atoms increased, while the relative atomic ratio of F to C was gradually decreased as the electron fluence increased (Figure 4 and Table S1 in the Supporting Information). For a detailed investigation of the change in molecular bonds, C 1s peaks of the pristine and electron-irradiated PTFE films were analyzed (Figure 5). The C 1s peak of the pristine PTFE film exhibited a sharp peak centered at 292.4 eV and a relatively small peak centered at 285.0 eV, indicating CF_2 and C—C bonds of C atoms, respectively. This result is obvious because the pristine PTFE has a chemical structure with the repeating unit of $-(\text{CF}_2-\text{CF}_2)-$. On the contrary, C 1s peaks of the electron-irradiated PTFE films showed broad peaks compared with that of the pristine PTFE film. The broad peaks of the electron-irradiated PTFE films were deconvoluted with several peaks representing C—C, C—O (286.5 eV), C=O (287.9 eV), C—F (290.0 eV), and CF_2 bonds. After electron irradiation of $5 \times 10^{16} \text{ cm}^{-2}$, the relative proportion of the CF_2 peak centered at 292.4 eV decreased, whereas that of the peak centered at 285.0 eV increased compared with the C 1s peak of the pristine PTFE, and a peak centered at 290.0 eV newly appeared. These results indicate that repeated CF_2 bonds of PTFE were decomposed into C—C and C—F bonds by the electron irradiation. Furthermore, additional bonds related to O atoms such as C—O and C=O, probably resulting from the interaction of carbon atoms with residual oxygen in the vacuum chamber, were produced. When the electron fluence was increased further, the CF_2 and C—F bonds were continuously decomposed, and the C—C bonds became more dominant. In addition, the number of C—O and C=O bonds generally increased as the electron fluence increased (see Table S2 in the Supporting Information).

The behavior of the CA change can be explained by the combined effect of the morphology and the chemical composition change as described above. The Wenzel model²⁷ is known to hold for slightly hydrophobic surfaces on which water droplets are strongly pinned.²⁸ According to the CAs of the films, water droplets on the films irradiated at an electron fluence of less than $2.5 \times 10^{16} \text{ cm}^{-2}$ are considered to be in the Wenzel state. As the electron fluence increased, the surface roughness continuously increased, as can be seen in the rms roughness data mentioned above (see also Figure S2 in the Supporting Information). Because a hydrophobic surface ($\text{CA} > 90^\circ$) becomes more hydrophobic with increasing the surface roughness according to the Wenzel model, the roughening of PTFE surfaces by the electron irradiation can result in an increase in CA. On the contrary, water droplets on the irradiated films, which are superhydrophobic, are considered to be in the Cassie state^{28,29} when the electron fluence is higher than $4 \times 10^{16} \text{ cm}^{-2}$. Besides, air trapping in the porous structures has a positive effect on the increase in CA according to the Cassie model. As can be seen in Figure 1 and Figure S2 in the Supporting Information, the pore size increased with increasing the electron fluence and thus leading to trapping of a greater amount of air. Thus, these results

reveal that the morphological change of PTFE films enhances the hydrophobic property whatever the state of water droplet is. However, a negative effect on the increase in CA simultaneously occurs because of the electron irradiation. The decomposition of hydrophobic CF_2 molecular bonds (defluorination) and the production of hydrophilic groups such as C=O bonds caused a decrease in CA.³⁰ Comprehensively, it seemed that the positive effect caused by the increase in surface roughness considerably outweighed the negative effect caused by the change of chemical composition until the electron fluence reached $6 \times 10^{17} \text{ cm}^{-2}$. Nevertheless, at an electron fluence of $1 \times 10^{18} \text{ cm}^{-2}$, it seemed that the total effect on the increase in CA became less positive because the surface roughness was not greatly increased compared to that of the $6 \times 10^{17} \text{ cm}^{-2}$ case (Figure 1e,f), and the surface became more defluorinated; hence, the CA decreased from $163.2 \pm 1.1^\circ$ to $154.2 \pm 1.7^\circ$. When the electron fluence was further increased to $2 \times 10^{18} \text{ cm}^{-2}$, the film did not even exhibit superhydrophobicity (CA: $136.4 \pm 1.2^\circ$, see Figure S1 in the Supporting Information). This result indicates that the wetting property of PTFE films can be precisely controlled and superhydrophobic surfaces can be obtained by the electron irradiation of PTFE films at a proper electron fluence.

CONCLUSIONS

A facile route to control the surface morphology and to fabricate superhydrophobic surfaces was presented based on the electron irradiation of PTFE films. After electron irradiation, rough surfaces with micrometer-sized pores were produced on the irradiated PTFE films. The formation of micrometer-sized pores was caused by the charging effect on the PTFE films during the electron irradiation, which brought about the local inhomogeneity of charge distribution, and thereby led to the inhomogeneous decomposition of the PTFE molecular chains by electron irradiation. By changing the electron fluence, the surface morphology of the PTFE films could be readily controlled. The change of chemical composition, including defluorination and oxidation, also occurred simultaneously with the change of surface morphology. Therefore, the wetting property could be precisely controlled by adjusting the electron fluence, and superhydrophobic surfaces were produced at a proper electron fluence. The electron irradiation approach presented here provides a promising tool to control the surface morphology and to fabricate superhydrophobic surfaces. The electron irradiation method is a one-step process, and no additional processes are required for the fabrication of superhydrophobic surfaces. Furthermore, the method might be successfully extended to fabricate superhydrophobic surfaces using other low-surface-energy materials including various fluoropolymers (see Figure S5 in the Supporting Information).

ASSOCIATED CONTENT

S Supporting Information. FESEM image of the PTFE film electron-irradiated at an electron fluence of $2 \times 10^{18} \text{ cm}^{-2}$; 3D surface profiles of the pristine and electron-irradiated PTFE films; Calculated penetration depth as a function of the electron energy; FESEM images of 50- μm -thick PTFE film irradiated with a 50-keV electron beam at an electron fluence of $6 \times 10^{17} \text{ cm}^{-2}$; FESEM images of electron-irradiated fluorinated ethylene propylene (FEP) and poly(tetrafluoroethylene-co-perfluoroalkyl vinyl ether) (PFA) films; Atomic concentrations at the pristine

and electron-irradiated PTFE surfaces measured by XPS; Integrated peak areas and percentage for deconvoluted C 1s spectra obtained by analyzing XPS C 1s peaks of the pristine and electron-irradiated PTFE films; Electrical charging phenomena monitored using a CCD camera. This material is available free of charge via the Internet at <http://pubs.acs.org/>.

■ AUTHOR INFORMATION

Corresponding Authors

*E-mail: jaehakchoi@kaeri.re.kr (J.-H. C.); socho@kaist.ac.kr (S. O. C.).

■ ACKNOWLEDGMENT

This work was supported by the Nuclear R&D Program of the National Research Foundation (NRF) funded by the Ministry of Education, Science and Technology (MEST), Republic of Korea.

■ REFERENCES

- (1) Marmur, A. *Annu. Rev. Mater. Res.* **2009**, *39*, 473–489.
- (2) Nyström, D.; Lindqvist, J.; Östmark, E.; Antoni, P.; Carlmark, A.; Hult, A.; Malmström, E. *ACS Appl. Mater. Interfaces* **2009**, *1*, 816–823.
- (3) Nimittrakoolchai, O.-U.; Supothina, S. *J. Eur. Ceram. Soc.* **2008**, *28*, 947–952.
- (4) Nakajima, A.; Hashimoto, K.; Watanabe, T. *Monatsh. Chem.* **2001**, *132*, 31–41.
- (5) Jucius, D.; Guobienė, A.; Grigaliūnas, V. *Appl. Surf. Sci.* **2010**, *256*, 2164–2169.
- (6) Li, J. *Polym. Compos.* **2010**, *31*, 38–42.
- (7) Hou, W.; Wang, Q. *J. Colloid Interface Sci.* **2009**, *333*, 400–403.
- (8) Zhang, J.; Li, J.; Han, Y. *Macromol. Rapid Commun.* **2004**, *25*, 1105–1108.
- (9) Jafari, R.; Menini, R.; Farzaneh, M. *Appl. Surf. Sci.* **2010**, *257*, 1540–1543.
- (10) Satyaprasad, A.; Jain, V.; Nema, S. K. *Appl. Surf. Sci.* **2007**, *253*, S462–S466.
- (11) Kwong, H. Y.; Wong, M. H.; Wong, Y. W.; Wong, K. H. *Appl. Surf. Sci.* **2007**, *253*, 8841–8845.
- (12) Burkarter, E.; Saul, C. K.; Thomazi, F.; Cruz, N. C.; Zanata, S. M.; Roman, L. S.; Schreiner, W. H. *J. Phys. D: Appl. Phys.* **2007**, *40*, 7778–7781.
- (13) Burkarter, E.; Saul, C. K.; Thomazi, F.; Cruz, N. C.; Raman, L. S.; Schreiner, W. H. *Surf. Coat. Technol.* **2007**, *202*, 194–198.
- (14) Chen, Y.; Zhao, Z.; Dai, J.; Liu, Y. *Appl. Surf. Sci.* **2007**, *254*, 464–467.
- (15) Spohr, R.; Sharma, G.; Forsberg, P.; Karlsson, M.; Hallén, A.; Westerberg, L. *Langmuir* **2010**, *26*, 6790–6796.
- (16) Vandencastele, N.; Nisol, B.; Viville, P.; Lazzaroni, R.; Castner, D. G.; Reniers, F. *Plasma Process. Polym.* **2008**, *5*, 661–671.
- (17) Kanda, K.; Ideta, T.; Haruyama, Y.; Ishigaki, H.; Matsui, S. *Jpn. J. Appl. Phys.* **2003**, *42*, 3983–3985.
- (18) Lee, E. J.; Lee, H. M.; Li, Y.; Hong, L. Y.; Kim, D. P.; Cho, S. O. *Macromol. Rapid Commun.* **2007**, *28*, 246–251.
- (19) Lee, E. J.; Kim, J. J.; Cho, S. O. *Langmuir* **2010**, *26*, 3024–3030.
- (20) Lee, H. M.; Kim, Y. N.; Kim, B. H.; Kim, S. O.; Cho, S. O. *Adv. Mater. (Weinheim, Ger.)* **2008**, *20*, 2094–2098.
- (21) Kwok, R. W. M. *XPS Peak Fitting Program for WIN95/98 XPSPEAK version 4.1*, Department of Chemistry, Chinese University of Hong Kong (Freeware), 2000.
- (22) Choi, J.-H.; Ganesan, R.; Kim, D.-K.; Jung, C.-H.; Hwang, I.-T.; Nho, Y.-C.; Yun, J.-M.; Kim, J.-B. *J. Polym. Sci., Part A: Polym. Chem.* **2009**, *47*, 6124–6134.
- (23) Liang, R. Q.; Su, X. B.; Wu, Q. C.; Fang, F. *Surf. Coat. Technol.* **2000**, *131*, 294–299.
- (24) Song, Z. G.; Ong, C. K.; Gong, H. *Appl. Surf. Sci.* **1997**, *119*, 169–175.
- (25) Johnson, R. E., Jr.; Dettre, R. H. *Adv. Chem. Ser.* **1964**, *43*, 112–135.
- (26) Yoshida, N.; Abe, Y.; Shigeta, H.; Takami, K.; Osaki, H.; Watanabe, T.; Hashimoto, K. *J. Sol–Gel Sci. Technol.* **2004**, *31*, 195–199.
- (27) Wenzel, R. N. *Ind. Eng. Chem.* **1936**, *28*, 998–994.
- (28) Lafuma, A.; Quéré, D. *Nat. Mater.* **2003**, *2*, 457–460.
- (29) Cassie, A. B. D.; Baxter, S. *Trans. Faraday Soc.* **1944**, *40*, 546–551.
- (30) Mandeville, J. S.; Tajmir-Riahi, H. A. *Biomacromolecules* **2010**, *11*, 465–472.